Research Paper
Computational Methods for Differential Equations
http://cmde.tabrizu.ac.ir
Vol. *, No. *, *, pp. 1-15
DOI:10.22034/cmde.2026.69094.3392

A rapid computation of the volume potential in boundary element methods

Laurent Tchoualag[1], Lionel Ouya Ndjansi[1,*], Jean Louis Woukeng[1], and Jean Daniel Mukam[2]

[1]Department of Computer Science and Mathematics, University of Dschang, P.O. Box 67, Dschang, Cameroon.

[2]Department of Mathematics, University of Wuppertal Gaussstrasse 20, 42119 Wuppertal, Germany.

Abstract

This work presents and analyzes a fast method for computing the volume potential using the Fast Fourier Transform (FFT) in combination with Gauss-Legendre and Gauss-Hammer quadrature rules, for both the Poisson equation and the linear elastostatic equation. Additionally, we provide corresponding error estimates and present numerical results that demonstrate the efficiency and reliability of the proposed algorithms.

Keywords. Boundary element methods, volume potential, FFT method, Gauss-Legendre and Gauss-Hammer quadrature rules.
2010 Mathematics Subject Classification. 65 NXX, 65 RXX..

1. Introduction

As technology advances, new fast and efficient algorithms for boundary element methods (BEM) [2, 3, 22], classical finite element methods (FEM) [11, 14], finite block methods (FBM) [1, 7, 12], and other numerical techniques continue to emerge for solving both homogeneous and inhomogeneous PDEs. The BEM, in particular, is well-suited for computational domains with complex boundaries. One of the reasons is that only the boundary domain is discretized, which makes it possible to have a discrete algebraic linear system with few unknowns, unlike the FEM, see e.g. [24, 27]. However, designing a sufficiently fast algorithm for the solution of inhomogeneous PDEs by the BEM is often not an easy task, as it requires a very rigorous computation technique of the volume or Newton potentials. Note that a direct standard method for the calculation of the volume potentials is possible but too cumbersome.

Over the past twenty years, several approaches have been proposed in the BEM community to handle this issue. In engineering and materials science, the dual reciprocity method (DRM) stands out as a frequently employed method, see [6, 21] and the references given therein. The technique of this method consists in transferring domain integrals to boundary integrals. Indeed, the key idea is to approximate the right-hand side of the PDE, for instance using radial basis functions (RBF) [8], which facilitates the computation of a particular solution. Additionally, this solution can be determined via finite element methods or finite difference methods [11, 25] by embedding the domain into an auxiliary domain and applying homogeneous Dirichlet boundary conditions to solve the inhomogeneous equation. A particular solution can also be obtained by using a fast multipole method (FMM) as in [4] or by applying a second-order Lubich discrete convolution quadrature as in [5]. Note that the recent advancements in volume potential evaluation have been made possible by leveraging the fast multipole method [9, 10, 13, 18–20, 24]. The central idea behind this method consists to split the computational domain into near and far fields, with a standard collocation approach used for points at the near field and the multipole expansion of the fundamental solution for points at the far field. In Addition, an error analysis is conducted and presented. This work introduces and examines a novel approach for efficiently and accurately evaluating the volume potential in BEM for mixed boundary value problem (MBVP), using the fast Fourier transform (FFT). This approach is an improvement of the results presented in [17, 23] for Poisson equation and linear elastostatic equation. Our approach is built on a particular mesh discretization of the circular

Received: 10 September 2025; Accepted: 30 April 2026.
∗ Corresponding author. Email: lndjansiouya@gmail.com.

domain, see, e.g., [15, 23]. Indeed, the domain is divided into M_r rings at each level of refinement. Each ring is divided into N adaptive elements and on each element, the volume potential is approximated by using the 4-points Gauss-Legendre or the 3-points Gauss-Hammer quadrature rules. Next, we can express the vector of volume potential over the ring as a sum of matrix-vector products. In addition, due to the circulant property of those matrices, the complexity for generating them is reduced from $\mathrm{O}(N^2)$ to $\mathrm{O}(N)$ (N represents the number of boundary elements) and the matrix-vector product is speed up by applying the FFT [17, 23, 26]. Finally, we focus on the theoretical Galerkin error, whereas errors arising from numerical approximations of the volume potential can be evaluated using Strang's Lemma [24], which maintains the optimal order of convergence.

This article have the following structure: Section 2 introduces the scalar MBVP of Poisson equation and derives the boundary integral equation (BIE). Section 3 focuses on the standard Galerkin procedure for the BIE formulated in section 2, examining the eigensystems of the involved operators and using one-periodical B-splines. Section 4 discusses the evaluation of the volume potential for the Poisson problem, as well as the associated Galerkin error. Section 5 presents numerical examples for the Poisson problems. Finally, section 6 extends the procedure developed in sections 3 and 4 to the linear elastostatics problem.

2. Poisson mixed boundary value problem and BIE

For a particular circular domain of $\mathbb{R}^2$, i.e., $\Omega \subset \mathbb{R}^2$, we examine the Poisson equation with mixed boundary value conditions as representative model problem:

$$-\Delta\Phi = g \text{ in } \Omega, \qquad \Phi = u_D \text{ on } \Gamma_D \quad \text{and} \quad \partial_n\Phi := \frac{\partial}{\partial n}\Phi = u_N \text{ on } \Gamma_N, \tag{2.1}$$

where n denotes the external unit normal to the boundary $\Gamma = \partial\Omega$, with Γ partitioned into two disjoint subsets Γ_D and Γ_N. As found in [22, 24], it follows that the solution Φ of Eq. (2.1) is

$$\Phi(x) = -\frac{1}{2\pi}\int_\Gamma \ln(|x-y|)\partial n_y\Phi(y)ds_y + \frac{1}{2\pi}\int_\Gamma \Phi(y)\partial n_y \ln(|x-y|)ds_y - \frac{1}{2\pi}\int_\Omega \ln(|x-y|)g(y)dy. \tag{2.2}$$

From the formula (2.2) one can remark that the solution Φ at a point $x \in \Omega$ is uniquely determined provided that the complete Cauchy data $[\Phi, \partial_n\Phi]_{|\Gamma}$ and the source term g are known. However, since the Cauchy data $[\Phi, \partial_n\Phi]_{|\Gamma}$ are only partially prescribed, with $\Phi|_{\Gamma_D} = u_D$ and $\partial_n\Phi|_{\Gamma_N} = u_N$, consequently we need to determine the missing data $\Phi|_{\Gamma_N}$ and $\partial_n\Phi|_{\Gamma_D}$. To achieve this, we follow the same approach as outlined in [15, 24] and easily construct the normal derivative as follows

$$\partial_n\Phi = S\Phi - Ng \quad \text{on } \Gamma, \tag{2.3}$$

where S is the Steklov-Poincaré operator given by

$$S = D + \left(\frac{1}{2}I + K'\right)V^{-1}\left(\frac{1}{2}I + K\right), \tag{2.4}$$

and Ng is the volume or Newton potential which satisfies

$$-Ng = -V^{-1}N_0g := N_1g - \left(\frac{1}{2}I + K'\right)V^{-1}N_0g \quad \text{on } \Gamma. \tag{2.5}$$

In Equations (2.4) and (2.5) we denote by $V : H^{-1/2}(\Gamma) \to H^{1/2}(\Gamma)$ the single layer integral operator, $K : H^{1/2}(\Gamma) \to H^{1/2}(\Gamma)$ the double layer integral operator, $K' : H^{-1/2}(\Gamma) \to H^{-1/2}(\Gamma)$ its adjoint, $D : H^{1/2}(\Gamma) \to H^{-1/2}(\Gamma)$ the hypersingular boundary integral operator, $N_0 : \tilde{H}^{-1}(\Omega) \to H^{1/2}(\Gamma)$ and $N_1 : \tilde{H}^{-1}(\Omega) \to H^{-1/2}(\Gamma)$ the volume potentials which are all defined for $x \in \Gamma$ as

$$(Vt)(x) = -\frac{1}{2\pi}\int_\Gamma t(y)\ln(|x-y|)\,ds_y, \qquad (Ku)(x) = -\frac{1}{2\pi}\int_\Gamma u(y)\frac{\partial}{\partial n_y}\ln(|x-y|)\,ds_y,$$
$$(K't)(x) = -\frac{1}{2\pi}\int_\Gamma t(y)\frac{\partial}{\partial n_x}\ln(|x-y|)\,ds_y, \quad (Du)(x) = \frac{1}{2\pi}\frac{\partial}{\partial n_x}\int_\Gamma u(y)\frac{\partial}{\partial n_y}\ln(|x-y|)\,ds_y,$$

$$(N_0 g)(x) = -\frac{1}{2\pi}\int_\Omega g(y)\ln(|x-y|)\,dy, \qquad (N_1 g)(x) = -\frac{1}{2\pi}\frac{\partial}{\partial n_x}\int_\Omega g(y)\ln(|x-y|)\,dy.$$

Note that $\tilde{H}^{-1}(\Omega)$ is the dual space of $H^1(\Omega)$ and all those above operators are bounded. In addition, the operators V and D satisfy the following notable assertions.

Lemma 2.1. *[24, Theorem 6.23 and 6.24] The boundary integral operators V and D are self-adjoint, and elliptic on $H^{-1/2}(\Gamma)$ and $H_*^{1/2}(\Gamma)$ respectively, that is,*

$$\langle Vt, t\rangle_\Gamma \geq c_1^V \parallel t \parallel^2_{H^{-1/2}(\Gamma)} \quad \text{for all} \quad t \in H^{-1/2}(\Gamma) \quad \text{and} \quad diam(\Omega) < 1,$$

with $c_1^V > 0$ and

$$\langle Dv, v\rangle_\Gamma \geq c_1^D \parallel v \parallel^2_{H^{1/2}(\Gamma)} \quad \text{for all} \quad v \in H_*^{1/2}(\Gamma) \quad \text{with} \quad c_1^D > 0,$$

where $H_*^{1/2}(\Gamma) = \{v \in H^{1/2}(\Gamma) : \langle v, \tilde{v}\rangle_\Gamma = 0$ for $\tilde{v} \in H^{-1/2}(\Gamma)\}$ with $\tilde{v}$ the natural density which satisfies an operator equation with a constraint,

$$(V\tilde{v})(x) = \lambda \quad \text{for } x \in \Gamma \text{ and } \lambda > 0, \qquad \langle \tilde{v}, 1\rangle_\Gamma = 1.$$

Note that the Steklov-Poincaré operator $S : H^{1/2}(\Gamma) \to H^{-1/2}(\Gamma)$ given by the representation in (2.4) is self–adjoint and $H_*^{1/2}(\Gamma)$-elliptic with the identical ellipticity estimate as the hypersingular boundary integral operator D, see, e.g., [24, p. 149, Eq. (6.46)], i.e.,

$$\langle S\mathrm{v}, \mathrm{v}\rangle_\Gamma \geq c_1^D \parallel \mathrm{v} \parallel^2_{H^{1/2}(\Gamma)} \quad \text{for all} \quad \mathrm{v} \in H_*^{1/2}(\Gamma). \tag{2.6}$$

Since our goal is to determine the unknown data $\Phi|_{\Gamma_N}$ and $\partial_n\Phi|_{\Gamma_D}$ to solve the problem (2.1), several boundary integral formulations can be used for this purpose, see, e.g. [18, 24]. In this work, we employ the formulation based on the Dirichlet to Neumann map (2.3) to determine $\Phi \in H^{1/2}(\Gamma)$ satisfying the given conditions [16, 17, 23]

$$\Phi = u_D \quad \text{on } \Gamma_D \quad \text{and} \quad \partial_n\Phi = S\Phi - Ng := u_N \quad \text{on } \Gamma_N. \tag{2.7}$$

Let set $\tilde{u}_D \in H^{1/2}(\Gamma)$ an appropriate extension of the given Dirichlet datum $u_D \in H^{1/2}(\Gamma_D)$ which satisfies $\tilde{u}_D|_{\Gamma_D} = u_D$. We then seek $\widehat{\Phi} := \Phi - \tilde{u}_D \in \tilde{H}^{1/2}(\Gamma_N)$ such that

$$\langle S\widehat{\Phi}, \mathrm{v}\rangle_{\Gamma_N} = \langle u_N + Ng - S\tilde{u}_D, \mathrm{v}\rangle_{\Gamma_N} \quad \text{for all } \mathrm{v} \in \tilde{H}^{1/2}(\Gamma_N). \tag{2.8}$$

Given that the Steklov–Poincaré operator $S : H^{1/2}(\Gamma) \to H^{-1/2}(\Gamma)$ is bounded and $\tilde{H}^{1/2}(\Gamma_N)$-elliptic, see, e.g., [24, p. 149, Eq. (6.48)], the existence of a unique solution to (2.8) is thereby established.

3. Boundary element methods

Prior to implementing the Galerkin discretization of the problem (2.8), it is necessary to find the eigensystems of the pertinent boundary operators involved in this equation.

3.1. **Eigensystems of the boundary operators.** For a given 2D circular domain $\Omega = B_R(O)$ (i.e., a disc centered at the origin and with radius R), with the boundary $\Gamma = \partial B_R(O)$ parametrized as

$$\partial B_R(O) := \left\{ x \in \mathbb{R}^2 : x(\eta) = R\left(\cos 2\pi\eta, \sin 2\pi\eta\right)^\top, \quad 0 \leq \eta < 1 \right\}, \tag{3.1}$$

it follows that the eigenfunctions of the single layer, double layer and hypersingular operators can be exactly computed as

$$(Vt)(\eta) = -R\int_0^1 \ln(2R|\sin\pi(\eta-\zeta)|)t(\zeta)d\zeta,$$

$$(Ku)(\eta) = -\frac{1}{2}\int_0^1 u(\zeta)d\zeta,$$

$$(Du)(\eta) = -\frac{1}{4R}\int_0^1 \frac{u(\zeta)}{\sin^2\pi(\eta-\zeta)}d\zeta.$$

Lemma 3.1. *[26, p. 3] Let the boundary Γ be given as in (3.1). The eigenfunctions of the boundary operators V, K and D are given by the Fourier functions*

$$v_k(\zeta) = e^{i2k\pi\zeta} \quad \text{for } k \in \mathbb{Z},$$

associated to the eigenvalues

$$\lambda_{V,k} = \begin{cases} -R\ln R, & \text{if } k = 0, \\ \dfrac{R}{2|k|}, & \text{if } k \neq 0, \end{cases} \quad \lambda_{K,k} = \begin{cases} -\frac{1}{2}, & \text{if } k = 0, \\ 0, & \text{if } k \neq 0, \end{cases} \quad \text{and} \quad \lambda_{D,k} = \frac{|k|}{2R},$$

for $k \in \mathbb{Z}$ respectively.

From the above Lemma 3.1, we remark that the eigenfunctions of the operator $\frac{1}{2}I + K$ is given by the functions $\mathrm{v}_k(\zeta) = e^{i2k\pi\zeta}$ associated to the eigenvalues

$$\lambda_{\frac{1}{2}I+K,k} = \begin{cases} 0, & \text{if } k = 0, \\ \frac{1}{2}, & \text{if } k \neq 0. \end{cases}$$

The next section presents the Galerkin method in the BEM to approximate solution of Equation (2.8).

3.2. **Galerkin boundary element formulation.** The standard Galerkin boundary element method provides a robust framework for numerically resolution the boundary integral equation (2.8) using one-periodic B-splines of order $n \geq 0$. By leveraging the parametrization of the boundary Γ given in (3.1), we discretize the interval $[0, 1)$ into $N > n + 1$ sub-intervals of uniform size $h = 1/N$, thereby obtaining

$$[0,1) = \bigcup_{\ell=1}^{N} [\zeta_\ell, \zeta_{\ell+1}), \quad \text{where } \zeta_\ell = (\ell - 1) \times h \quad \forall \ell = 1, ..., N + 1.$$

Additionally, we denote by $\mathbb{S}_N^n$ the subspace of one-periodic functions, i.e., $\mathbb{S}_N^n = \mathrm{Span}\big(\varphi_1^{(n)}(\zeta), ..., \varphi_N^{(n)}(\zeta)\big)$, where $\varphi_k^{(n)}(\zeta)$ with $k = 1, ..., N$ are the B-splines of order n defined recursively as follows (see e.g., [15, 17])

$$\varphi_1^{(0)}(\zeta) = \begin{cases} 1, & -h/2 \leq \zeta < h/2, \\ 0, & -1/2 \leq \zeta < -h/2 \quad \text{or} \quad h/2 \leq \zeta < 1/2, \end{cases} \tag{3.2}$$

$$\varphi_1^{(n)}(\zeta) = \frac{1}{h} \int_{-1/2}^{1/2} \varphi_1^{(n-1)}(\eta)\varphi_1^{(0)}(\zeta - \eta)d\eta \quad \text{for all } n = 1, 2, ..., \tag{3.3}$$

and

$$\varphi_k^{(n)}(\zeta) = \varphi_1^{(n)}(\zeta - (k-1) \times h) \text{ for all } k = 1, ..., N \quad \text{with} \quad \varphi_k^{(n)}(\zeta + m) = \varphi_k^{(n)}(\zeta) \quad \forall m \in \mathbb{Z}.$$

We further employ the Fourier series representation of the basis functions $\varphi_\ell^{(n)}$, which is given by

$$\varphi_\ell^{(n)}(\zeta) = \sum_{k\in\mathbb{Z}} c_\ell^n(k) e^{i2\pi k\zeta}, \quad \ell = 1, ..., N, \quad n = 0, 1, ..., \tag{3.4}$$

with the Fourier coefficients given explicitly as [15, 17]

$$c_1^n(k) = \begin{cases} h, & \text{if } k = 0, \\ \dfrac{\sin^{n+1}(k\pi h)}{k\pi(k\pi h)^n}, & \text{if } k \neq 0, \end{cases} \quad \text{and} \quad c_\ell^n(k) = c_1^n(k)e^{-i2\pi kh(\ell-1)} \qquad \forall \ell = 1, ..., N.$$

To simplify the presentation, we set $n = 1$ in the rest of this document. Next, the equivalent Galerkin formulation of Eq. (2.8) consists of finding $\widehat{\Phi}_h \in \mathbb{S}_N^1 \cap \tilde{H}^{1/2}(\Gamma_N)$ such that

$$\langle S\widehat{\Phi}_h, \mathrm{v}_h\rangle_{\Gamma_N} = \langle u_N - S\tilde{u}_D, \mathrm{v}_h\rangle_{\Gamma_N} + \langle Ng, \mathrm{v}_h\rangle_{\Gamma_N} \quad \text{for all } \mathrm{v}_h \in \mathbb{S}_N^1 \cap \tilde{H}^{1/2}(\Gamma_N). \tag{3.5}$$

From (2.6) and the Lax-Milgram Lemma, we deduce that, the discret formulation (3.5) has a unique solution. Furthermore, applying Lemma of Cea and using the approximation property of $\mathbb{S}_N^1$ [24, p. 241, Theorem 10.9], we derive the error estimates

$$\|\widehat{\Phi}-\widehat{\Phi}_h\|_{H^{1/2}(\Gamma)} \leq ch^{3/2}|\Phi|_{H^2(\Gamma)} \quad \text{and} \quad \|\widehat{\Phi}-\widehat{\Phi}_h\|_{L^2(\Gamma)} \leq ch^2|\Phi|_{H^2(\Gamma)}, \tag{3.6}$$

provided that $\Phi \in H^2(\Gamma)$.

In addition, the boundary element formulation of (3.5) can be written equivalently as the system of linear equations

$$S_h\underline{\widehat{\Phi}} = \underline{g}_1 + \underline{g}_2, \tag{3.7}$$

whereby S_h denotes the stiffness matrix

$$S_h[\ell,j] = \langle S\varphi_j^{(1)}, \varphi_\ell^{(1)}\rangle_{\Gamma_N} \quad \text{for } \ell,j = 1,...,M := \dim\big(\mathbb{S}_N^1 \cap \tilde{H}^{1/2}(\Gamma_N)\big),$$

and the right-hand side components are

$$\underline{g}_1[\ell] = \langle u_N - S\tilde{u}_D, \varphi_\ell^{(1)}\rangle_{\Gamma_N} \text{ and } \underline{g}_2[\ell] = \langle Ng, \varphi_\ell^{(1)}\rangle_{\Gamma_N} \quad \text{for } \ell = 1,...,M,$$

where $Ng = V^{-1}N_0 g$.

For the Poisson equation, the Galerkin discretization of the Steklov-Poincaré operator can be explicitly constructed using its eigenfunctions. However, our focus on using the discrete Fourier matrix as a preconditioner leads us to define a symmetric approximation of the continuous Steklov-Poincaré operator S. To achieve this, we first introduce the Galerkin discretizations of the boundary operators V, K, K' and D which are given by:

$$V_h[\ell,j] = \langle V\varphi_j^{(0)}, \varphi_\ell^{(0)}\rangle_\Gamma, \quad \hat{K}_h[\ell,j] = \langle (\frac{1}{2}I + K)\varphi_j^{(1)}, \varphi_\ell^{(0)}\rangle_\Gamma,$$
$$D_h[\ell,k] = \langle D\varphi_k^{(1)}, \varphi_\ell^{(1)}\rangle_\Gamma \quad \forall \ell,j = 1,...,N.$$

The above matrices can be calculated explicitly and efficiently by exploiting the next Lemma, where the proof can be found in [26].

Lemma 3.2. *Consider Γ as defined in (3.1). The matrices V_h, $\hat{K}_h$ and D_h, exhibit circulant matrix structures. Furthermore, V_h and D_h are symmetric and positive definite, and the eigenvalues of all these matrices are given respectively by*

$$\lambda_{V_{h,j}} = \begin{cases} -Rh\ln(R), & \text{for } j = 1, \\ \frac{1}{2}h^2R\left(\frac{\sin(\pi\zeta)}{\pi}\right)^2 \sum_{k=0}^{\infty}\left[\frac{1}{(k+\zeta)^3} + \frac{1}{(k-\zeta+1)^3}\right], & \text{for } j \geq 2, \end{cases}$$

$$\lambda_{\hat{K}_{h,j}} = \begin{cases} 0, & \text{for } j = 1, \\ \frac{1}{2}h\left(\frac{\sin(\pi\zeta)}{\pi}\right)^3 \sum_{k=0}^{\infty}\left[\frac{(-1)^k}{(k+\zeta)^3} + \frac{(-1)^k}{(k-\zeta+1)^3}\right], & \text{for } j \geq 2, \end{cases}$$

$$\lambda_{D_{h,j}} = \begin{cases} 0, & \text{for } j = 1, \\ \frac{1}{2R}\left(\frac{\sin(\pi\zeta)}{\pi}\right)^4 \sum_{k=0}^{\infty}\left[\frac{1}{(k+\zeta)^3} + \frac{1}{(k-\zeta+1)^3}\right], & \text{for } j \geq 2, \end{cases}$$

for $\zeta = h(j-1)$ and $h = \frac{1}{N}$ respectively.

One of the most significant properties of the circulant matrices is that they are diagonalizable and admit straightforward inversion, provided the inverse exists. Using the Fourier matrices $Q \in \mathbb{R}^{N\times N}$ and $F \in \mathbb{C}^{N\times N}$, we can decompose the matrices of the discrete boundary operators as follows

$$V_h = N^{-1}QD_{V_h}Q, \quad \hat{K}_h = N^{-1}FD_{\hat{K}_h}F^*, \quad D_h = N^{-1}QD_{D_h}Q,$$

where

$$F[k,\ell] = e^{i2\pi h(k-1)(\ell-1)}, \quad Q[k,\ell] = \cos[2\pi h(k-1)(\ell-1)] + \sin[2\pi h(k-1)(\ell-1)],$$

for $k,\ell = 1,...,N$, and the diagonal matrices D_{V_h}, $D_{\hat{K}_h}$ and D_{D_h} are determined by the eigenvalues of V_h, $\hat{K}_h$ and D_h respectively.

Next, we approximate the operator S by

$$\tilde{S}_h := D_h + \hat{K}_h^\top V_h^{-1} \hat{K}_h. \tag{3.8}$$

and therefore, the boundary formulation (2.8) takes the equivalent form

$$\tilde{S}_h \underline{\tilde{\Phi}} = \underline{g}_1 + \underline{g}_2. \tag{3.9}$$

Observe that $\tilde{S}_h$ provides a positive definite approximation of S_h, with an additional error analyzable through Strang's Lemma [24]. Furthermore, $\tilde{S}_h$ is defined on the whole boundary Γ, but applies only to $\underline{\tilde{\Phi}} \leftrightarrow \tilde{\Phi}_h \in \mathbb{S}_N^1 \cap \tilde{H}^{1/2}(\Gamma_N)$ easily handled in iterative solvers.

Evaluation of the vector $\underline{g}_2$ in Eq. (3.9), resulting from the volume potential Ng, remains to be analyzed in detail. For this fact, we will use circulant matrices for their efficiency in matrix-vector multiplications and memory storage. Indeed, by taking $\ell = 1,...,M$ and using Eq. (2.5) we can write the components of the vector $\underline{g}_2$ as follows

$$\underline{g}_2[\ell] = \langle Ng, \varphi_\ell^{(1)} \rangle_{\Gamma_N} = \langle V^{-1} N_0 g, \varphi_\ell^{(1)} \rangle_{\Gamma_N}. \tag{3.10}$$

Note that the variational formulation

$$\langle Vw, z \rangle_\Gamma = \langle N_0 g, z \rangle_\Gamma \quad \text{for all} \quad z \in H^{-1/2}(\Gamma). \tag{3.11}$$

has a unique solution given by $w = V^{-1} N_0 g \in H^{-1/2}(\Gamma)$. Furthermore, for the Galerkin formulation of the problem (3.11), we seek $w_h \in \mathbb{S}_N^0$ satisfying

$$\langle Vw_h, z_h \rangle_\Gamma = \langle N_0 g, z_h \rangle_\Gamma \quad \text{for all} \quad z_h \in \mathbb{S}_N^0. \tag{3.12}$$

Consequently, the volume potential

$$N_0 g[\ell] = \int_\Gamma \varphi_\ell^{(0)}(x) \int_\Omega U^*(x,y) g(y) \; dy ds_x \quad \text{for } \ell = 1,...,N, \tag{3.13}$$

need to be determined efficiently as the right hand side of (3.12), where $U^*(x,y) = -\frac{1}{2\pi} \ln|x-y|$. This will enable us to define an approximate right hand side $\tilde{\underline{g}}_2$ with an additional error evaluated via Strang's Lemma, while maintaining optimal order of convergence as in [24].

4. Volume potential for the Poisson problem

4.1. **By using interpolations and quadrature rules.** In this section, we discuss an efficient evaluation of the volume potential (3.13). Using piecewise constant basis functions, the discrete volume potential $N_0 g[\ell]$ is computed by first interchanging the order of integration, as follows:

$$N_0 g[\ell] = \int_\Omega g(y) \int_{\tau_\ell} U^*(x,y) \; ds_x dy.$$

Further, a sophisticated adaptive mesh methodology is employed in the domain Ω, where the domain is first partitioned into M_r annular regions, and adaptive grids are generated on each ring. Next, the mesh size of the volume elements near the boundary is assumed to be the same as for the boundary elements, that is, $r_1 = \vartheta$. Moreover, from the rings close to the boundary to the inner rings the size is reduced with the rate $0 < q < 1$ such that for $j = 1,...,M_r - 1$ the relation $r_{j+1} = q r_j$ holds as we move from the boundary to the interior, as illustrated in Figure 1.

Furthermore, note that the values of q can be obtained by solving the equation

$$q^{M_r} - \frac{N}{2\pi} q + \frac{N - 2\pi}{2\pi} = 0 \quad \text{with} \quad q \neq 1, \tag{4.1}$$

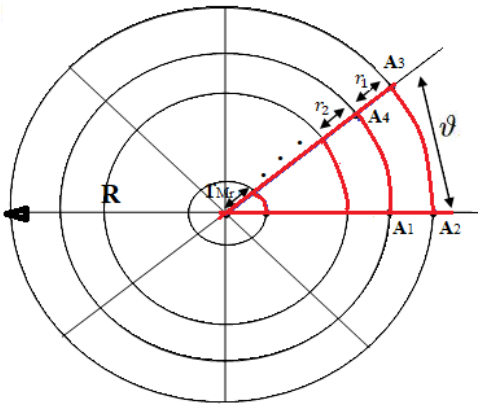

FIGURE 1. Volume and boundary meshes.

for the given values of M_r (number of rings) and N (number of elements on each ring). Equation (4.1) follows from the fact that the radius of the disc is

$$R := \sum_{j=1}^{M_r} r_j = \sum_{j=1}^{M_r} q^{j-1}\vartheta = \vartheta\frac{1-q^{M_r}}{1-q} \quad \text{for} \quad q \neq 1 \quad \text{and} \quad \vartheta = \frac{2\pi R}{N}.$$

From these above results, we then obtain

$$N_0 g[\ell] = \sum_{k=1}^{M_r}\sum_{j=1}^{N} \int_{T_{kj}} g(y) \int_{\tau_\ell} U^*(x,y)\, ds_x dy, \tag{4.2}$$

where T_{kj} is an isoparametric quadrangle, except for the last inner ring, where it is an isoparametric triangle. Observe that $\overline{\Omega} = \cup_{k=1}^{M_r}\cup_{j=1}^{N} T_{kj}$, with N also being the number of boundary elements. Then, an approximation of (4.2) is given by using first, the $\mathcal{P}_2$-iterpolation on isoparametric triangle and the Q_2-interpolation on isoparametric quadrangle respectively. Second, the 3-points Gauss-Hammer and the 4-points Gauss-Legendre quadrature rules are used to approximate the integral we obtain on isoparametric triangle and isoparametric quadrangle respectively, see Figure 2.

We then obtain

$$N_0 g[\ell] = \sum_{k=1}^{M_r}\sum_{j=1}^{N} \int_{\bar{T}_{kj}} \left(g\big(\psi(\varepsilon,\lambda)\big)|J_\psi(\varepsilon,\lambda)| \int_{\tau_\ell} U^*\big(x,\psi(\varepsilon,\lambda)\big)\, ds_x \right) d\varepsilon d\lambda, \tag{4.3}$$

for $\ell = 1, \cdots, N$, where $|J_\psi(\varepsilon,\lambda)|$ is the Jacobian. This formula (4.3) leads to

$$\tilde{N}_0 g[\ell] = \sum_{k=1}^{M_r}\sum_{j=1}^{N}\sum_{i=1}^{\mathcal{I}} w_{kj}^i |J_\psi(\varepsilon_i,\lambda_i)| \Pi_h g\big(G_{kj}^i\big) \int_{\tau_\ell} U^*\big(x, G_{kj}^i\big)\, ds_x, \tag{4.4}$$

where w_{kj}^i and G_{kj}^i represent the weight and the point of the Gauss quadrature on the element T_{kj}, respectively, and Π_h denotes the interpolation operator defined by $\Pi_h : \mathcal{C}(\overline{\Omega}) \to L^2(\Omega)$ such that $\Pi_h v|_{T_{kj}} = \Pi_{T_{kj}} v$, where $\Pi_{T_{kj}}$ represents the interpolation operator associated to the element T_{kj}. The remaining boundary integral is handled by discretizing the single layer potential using the collocation method, a numerical approach that facilitates efficient and accurate computation of the integral. If we reorganize (4.4) as follows

$$\tilde{N}_0 g[\ell] = \sum_{k=1}^{M_r}\sum_{i=1}^{\mathcal{I}}\sum_{j=1}^{N} w_{kj}^i \big|J_\psi\big(\varepsilon_i,\lambda_i\big)\big| \Pi_h g\big(G_{kj}^i\big) \int_{\tau_\ell} U^*\big(x, G_{kj}^i\big)\, ds_x, \tag{4.5}$$

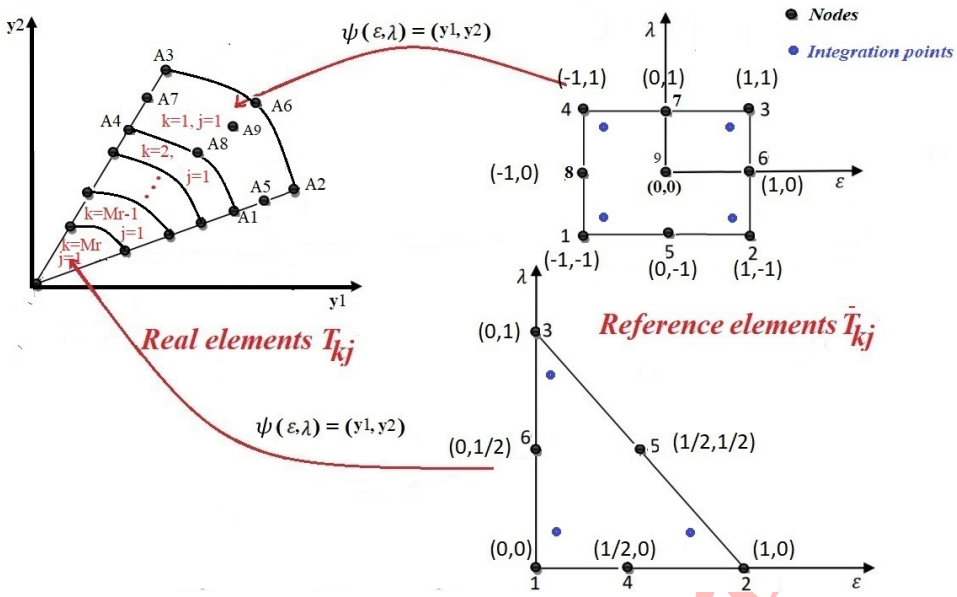

FIGURE 2. Isoparametric configuration.

for $\ell = 1, ..., N$, we then obtain from (4.5) that the vector $\tilde{N}_0 g$ can be expressed in the following matricial form

$$\underline{\tilde{N}}_0 g := \sum_{k=1}^{M_r} \sum_{i=1}^{\mathcal{I}} A_{ki} \underline{F}_{ki}, \tag{4.6}$$

where $\underline{F}_{ki}$ and A_{ki} for $k = 1, 2, ..., M_r$, $i = 1, 2, ..., \mathcal{I}$ are the vector and the matrix defined by

$$\underline{F}_{ki}[j] = w^i_{kj} |J_\psi(\varepsilon_i, \lambda_i)| \Pi_h g(G^i_{kj}) \quad \text{for } j = 1, ..., N, \tag{4.7}$$

and

$$A_{ki}[\ell, j] = \int_{\tau_\ell} U^*(x, G^i_{kj}) ds_x \quad \text{for } \ell, j = 1, ..., N. \tag{4.8}$$

We note that, for ring number k, there exist $\mathcal{I}$ vectors $\underline{F}_{ki}$ and $\mathcal{I}$ corresponding matrices A_{ki}. In addition, given the uniform meshes on the boundary as well as on each rings, combined to the invariance of the fundamental solution $U^*(.,.)$ with respect to rotations, and the fact that $G^i_{k(j+1)}$ and $\tau_{\ell+1}$ are the images by the rotation with respect to the angle $2\pi h$ of G^i_{kj} and τ_ℓ respectively, we then obtain

$$A_{ki}[\ell + 1, j + 1] = A_{ki}[\ell, j] \quad \text{for } \ell, j = 1, ..., N, \tag{4.9}$$

therefore, the matrices A_{ki} are circulant. This leads to a significant reduction in computational effort, from $O(N^2)$ to $O(N)$ for generating the matrix A_{ki}, since only the first row or the column is computed, and from $O(N^2)$ to $O\big(N \log(N)\big)$ for matrix-vector multiplication when FFT is applied, see, e.g., [15, 17, 23]. Furthermore, by using piecewise constant basis functions $\varphi^{(0)}_\ell$, $\ell = 1, ..., N$ in the Galerkin formulation (3.12), we are led to determine an approximation $\tilde{w}_h \in \mathbb{S}^0_N$ which is a unique solution of the following Galerkin formulation

$$\langle V \tilde{w}_h, \varphi^{(0)}_\ell \rangle_\Gamma = \langle \tilde{N}_0 g, \varphi^{(0)}_\ell \rangle_\Gamma. \tag{4.10}$$

The Garlerkin formulation (4.10) leads to the linear system given by

$$V_h \underline{\tilde{w}} = \underline{\tilde{N}}_0 g, \tag{4.11}$$

where V_h is the stiffness matrix of the single layer, while $\underline{\tilde{N}}_0 g$ is the discrete approximation of the volume potential given by (4.6). Since V_h is a circulant matrix and $\underline{\tilde{N}}_0 g$ a sum of matrix-vector products with circulant matrices, the linear system (4.11) can be solved very efficiently by using FFT, and the solution is given by

$$\underline{\tilde{w}} = \sum_{k=1}^{M_r} \sum_{i=1}^{\mathcal{I}} \mathcal{F}^{-1}\left(\frac{\mathcal{F}(C_{ki})\mathcal{F}(\underline{F}_{ki})}{\Lambda_h}\right), \tag{4.12}$$

where $\mathcal{F}$ is the discrete FFT and $\mathcal{F}^{-1}$ its inverse, Λ_h and C_{ki} are the vectors of the eigenvalues of the matrix V_h and the first column of the matrix A_{ki} respectively.

4.2. **Error estimates.** Owing to the evaluation of the volume potential via interpolations and quadrature rules in section 4.1, we must consider a following perturbed variational problem in place of (3.5) to seek $\tilde{\Phi}_h \in \mathbb{S}_N^1 \cap \tilde{H}^{1/2}(\Gamma_N)$

$$\langle S\tilde{\Phi}_h, \mathrm{v}_h\rangle_{\Gamma_N} = \langle u_N - S\tilde{u}_D, \mathrm{v}_h\rangle_{\Gamma_N} + \langle \tilde{w}_h, \mathrm{v}_h\rangle_{\Gamma_N} \text{ for } \mathrm{v}_h \in \mathbb{S}_N^1 \cap \tilde{H}^{1/2}(\Gamma_N), \tag{4.13}$$

where $\tilde{w}_h = V^{-1}\tilde{N}_0 g$. Therefore, the error $\widehat{\Phi}_h - \tilde{\Phi}_h$ resulting from the perturbation of the right-hand side needs to be estimated. By replacing the second term of the right-hand side of (3.5) by $\langle w_h, \mathrm{v}_h\rangle_{\Gamma_N}$ for all $\mathrm{v}_h \in \mathbb{S}_N^1 \cap \tilde{H}^{1/2}(\Gamma_N)$, subtracting (4.13) from (3.5) and by using the ellipticity (2.6) of Steklov-Poincaré S we then obtain

$$\|\widehat{\Phi}_h - \tilde{\Phi}_h\|_{H^{1/2}(\Gamma)} \leq c\|w_h - \tilde{w}_h\|_{H^{-1/2}(\Gamma)} \tag{4.14}$$

with a constant c independent from h. In addition, we also consider the perturbed Galerkin formulation instead of (3.12) seeking $\tilde{w}_h \in \mathbb{S}_N^0$ that satisfies

$$\langle V\tilde{w}_h, z_h\rangle_\Gamma = \langle \tilde{N}_0 g, z_h\rangle_\Gamma \text{ for } z_h \in \mathbb{S}_N^0. \tag{4.15}$$

By subtracting (4.15) from (3.12), and by setting $z_h = w_h - \tilde{w}_h$ and by using the ellipticity of V, this yields

$$c_1^V \|w_h - \tilde{w}_h\|^2_{H^{-1/2}(\Gamma)} \leq \|N_0 g - \tilde{N}_0 g\|_{L^2(\Gamma)}\|w_h - \tilde{w}_h\|_{L^2(\Gamma)}.$$

By using the inverse inequality in $\mathbb{S}_N^0$ we have

$$\|w_h - \tilde{w}_h\|_{L^2(\Gamma)} \leq c_I h^{-1/2}\|w_h - \tilde{w}_h\|_{H^{-1/2}(\Gamma)}.$$

Thus, we obtain

$$\|w_h - \tilde{w}_h\|_{H^{-1/2}(\Gamma)} \leq \frac{c_I}{c_1^V} h^{-1/2}\|N_0 g - \tilde{N}_0 g\|_{L^2(\Gamma)}. \tag{4.16}$$

By using (4.14) and (4.16) we then obtain

$$\|\widehat{\Phi}_h - \tilde{\Phi}_h\|_{H^{1/2}(\Gamma)} \leq ch^{-1/2}\|N_0 g - \tilde{N}_0 g\|_{L^2(\Gamma)}. \tag{4.17}$$

But we have

$$\begin{aligned}
\|N_0 g - \tilde{N}_0 g\|^2_{L^2(\Gamma)} &= \int_\Gamma \big(N_0 g(x) - \tilde{N}_0 g(x)\big)^2 ds_x \\
&= \int_\Gamma \left(\int_\Omega U^*(x,y)\big(g(y) - \Pi_h g(y)\big)dy\right)^2 ds_x \\
&\leq \|U^*\|^2_{L^2(\Gamma\times\Omega)}\|g - \Pi_h g\|^2_{L^2(\Omega)}.
\end{aligned}$$

Hence

$$\|\widehat{\Phi}_h - \tilde{\Phi}_h\|_{H^{1/2}(\Gamma)} \leq ch^{5/2}\|U^*\|_{L^2(\Gamma\times\Omega)}|g|_{H^3(\Omega)}. \tag{4.18}$$

provided that $g \in H^3(\Omega)$. By using the triangle inequality, Equations (3.6) and (4.18) we then obtain

$$\|\widehat{\Phi} - \tilde{\Phi}_h\|_{H^{1/2}(\Gamma)} \leq \hat{c}h^{3/2} \quad \text{with } \hat{c} > 0. \tag{4.19}$$

5. Numerical examples

As a numerical example, we consider Poisson's equation

$$-\triangle\Phi(x_1, x_2) = -(2 + x_2^2)\exp(x_1) \text{ in } \Omega, \tag{5.1}$$

where we suppose $\Omega = \mathcal{B}_R(c)$ to be a disc centered at $c = (0.4, 0.4)^\top$ with radius $R = 0.4$. The Neumann boundary Γ_N corresponds to the arc of the disc between 0 and $\pi/2$, while the Dirichlet boundary Γ_D is the complement $\Gamma\backslash\Gamma_N$. In addition, the exact solution of the given problem (5.1) is $\Phi(x_1, x_2) = x_2^2\exp(x_1)$. Next, the efficient evaluation of the volume potential is done by a suitable discretization of the domain Ω presented in section 4. For the given values of M_r (number of rings) as well as N (number of elements on Γ), we first determine the values of the rate q by solving Equation (4.1) with the Newton-Raphson method, see Table 1.

Table 1. Computation of the values of q from the known values of N and M_r.

N	Minimum value of M_r	Value of the rate q
04	impossible	impossible
08	02	0.2732395447
16	03	0.8403279783
32	06	0.9340030299
64	11	0.9844995556
128	21	0.9969506357
256	41	0.9996861199
512	82	0.9998449893
1024	163	0.9999229681
2048	326	0.9999990433
4096	653	0.9999995224

In the next step, we determine the vector of Newton potential $w = V^{-1}N_0 f$ associated to the right-hand side of the linear system (3.9), by using the efficient method that we develop in formula (4.12), see the Table 2 for the results.

In the Table 2, the first and second columns list the number of elements and rings, respectively. The third and the fourth columns represent the time (in seconds) needed to compute the vector $w = V^{-1}N_0 f$ by using the method (4.12) and the direct method respectively.

Table 2. Time to compute $w = V^{-1}N_0 f$ with two (02) different methods.

		Time to compute $w = V^{-1}N_0 f$	
N	M_r	By using method (4.12)	By using direct method
128	41	1.1731×10^{-2}	1.44×10^{-2}
256	82	4.043×10^{-2}	6.5×10^{-2}
512	163	0.128417	0.49
1024	326	0.419074	3.68
2048	654	1.63	25.05

From the results in the Table 2, we can observe that, when N doubles, the time to compute the Newton potential by using the method (4.12) is multiplied by four (04), which means a quadratic complexity, which is even better than what expected from the theory ($O(N^2 \log N)$) since the number of rings (M_r) is almost equals to $\frac{N}{4}$. But we observe a cubic complexity when the direct method is used.

We conclude this section by presenting the results of the resolution of the linear system (3.9), when the Conjugate gradient (CG) methods with preconditioner and without preconditioner are used. Note that the preconditioning matrix

used is $\mathbf{C}_D := \bar{\mathbf{M}}_h \bar{\mathbf{V}}_h^{-1} \bar{\mathbf{M}}_h$, where $\bar{\mathbf{V}}_h$ is the discrete single layer matrix and $\bar{\mathbf{M}}_h$ is the mass matrix, constructed by using piecewise linear B-splines, see e.g. in [17, 26] and the references given therein. In table 3, the third and the fourth columns represent the number of iterations for the CG method with preconditioner (#iter1) and the CG method without preconditioner (#iter2) respectively. The fifth and seventh columns represent the L^2 norms of $\Phi - \Phi_h$ and $t - t_h$ respectively. The sixth and eight columns give the estimate order of convergence, which confirm the expected theoretical results.

TABLE 3. The L^2 errors, estimate order of convergence and number of iterations.

		Iterations		L^2 **error of** u **and eoc.**		L^2 **error of** $t = \partial_n u$ **and eoc.**	
N	M_r	#iter1	#iter2	$\|\Phi - \Phi_h\|_{L^2(\Gamma)}$	eoc	$\|t - t_h\|_{L^2(\Gamma)}$	eoc
128	41	12	19	1.026×10^{-4}		0.03289	
256	82	13	27	2.56×10^{-5}	2.0028	0.01645	0.9996
512	163	13	40	6.40×10^{-6}	2.0000	8.2254×10^{-3}	0.9999
1024	326	13	58	1.60×10^{-6}	2.0000	4.11275×10^{-3}	1.0000
2048	654	13	83	4×10^{-7}	2.0000	2.0563×10^{-3}	1.0000
The expected theoretical results					**2**		**1**

6. Linear elastostatics problems

6.1. **MBVP in linear elasticity.** In this section, a simply connected domain $\Omega \subset \mathbb{R}^2$ of elastic body is considered. The vector $\underline{\Phi}(x)$ represents the displacement field and satisfies the following isotropic, inhomogeneous, ideal elastostatics equations with the mixed boundary value problem

$$-\mu\triangle\underline{\Phi} - (\lambda+\mu)\text{grad div } \underline{\Phi} = \underline{g} \text{ in } \Omega, \quad \underline{\Phi} = \underline{u}_D \text{ on } \Gamma_D \quad \text{and} \quad T_x(\underline{\Phi}) = \underline{u}_N \text{ on } \Gamma_N, \tag{6.1}$$

where $T_x(.) := \gamma_{1,x}^{int}(.)$ represents the boundary stress operator, $\triangle$ is the Laplacian and $\mu > 0$, $\lambda > 2\mu/3$ denote the Lamé constants. By the following Betti representation formula [15, 22, 27], we derive the solution $\underline{\Phi}$ of the PDE in (6.1) for all $x \in \Omega$ ($x \notin \Gamma$),

$$\underline{\Phi}(x) = \int_\Gamma U^*(x,y)\gamma_{1,y}^{int}\underline{\Phi}(y)ds_y - \int_\Gamma [T_y U^*(x,y)]^\top \gamma_{0,y}^{int}\underline{\Phi}(y)ds_y + \int_\Omega U^*(x,y)\underline{g}(y)dy, \tag{6.2}$$

where $U^*(x,y)$ denotes the fundamental solution of the partial differential operator of the linear elasticity in two dimension given by

$$U^*(x,y) = \alpha \log|x-y|.I + \beta\frac{(x-y)(x-y)^\top}{|x-y|^2}, \quad \alpha = -\frac{1}{4\pi}\frac{1}{\mu}\frac{\lambda+3\mu}{\lambda+2\mu}, \quad \beta = -\alpha\frac{\lambda+\mu}{\lambda+3\mu},$$

and for any vector $\underline{\mathrm{v}} = (\mathrm{v}_1, \mathrm{v}_2)^\top$, the boundary stress $T_y(.)$ is expressed as follows

$$(T_y\,\underline{\mathrm{v}})^\top = \lambda \text{ div } \underline{\mathrm{v}}\,\underline{n}(y) + 2\mu\,\frac{\partial\underline{\mathrm{v}}}{\partial\underline{n}} + \mu\left(n_2\frac{\partial \mathrm{v}_2}{\partial y_1} - n_2\frac{\partial \mathrm{v}_1}{\partial y_2}\,,\; n_1\frac{\partial \mathrm{v}_1}{\partial y_2} - n_1\frac{\partial \mathrm{v}_2}{\partial y_1}\right)^\top, \tag{6.3}$$

where $\underline{n}(y) := (n_1, n_2)^\top$ represents external unit normal at $y \in \Gamma$.

In the same way as in Section 2, we derive the variational formulation of (6.1) as follows: seek $\widehat{\underline{\Phi}} := \underline{\Phi} - \underline{\tilde{u}}_D \in (\tilde{H}^{1/2}(\Gamma_N))^2$ satisfiying

$$\langle S\widehat{\underline{\Phi}}, \underline{v}\rangle_{\Gamma_N} = \langle \underline{u}_N + N\underline{g} - S\underline{\tilde{u}}_D, \underline{v}\rangle_{\Gamma_N} \text{ for all } \underline{v} \in (\tilde{H}^{1/2}(\Gamma_N))^2, \tag{6.4}$$

where $\underline{\tilde{u}}_D \in (H^{1/2}(\Gamma))^2$ represents an arbitrary but fixed extension of the Dirichlet datum $\underline{u}_D \in (H^{1/2}(\Gamma_D))^2$ such that $\underline{\tilde{u}}_D(x) = \underline{u}_D(x)$ for $x \in \Gamma_D$. Furthermore, since the Steklov-Poincaré operator $S : \left(H^{1/2}(\Gamma)\right)^2 \to \left(H^{-1/2}(\Gamma)\right)^2$ is

bounded, self-adjoint, positive semi-definite and $(\tilde{H}^{1/2}(\Gamma_N))^2-$elliptic [17, 24], the existence of a unique solution to (6.4) can be easily shown. In addition, as in Section 3.2, the Galerkin formulation of the problem (6.4) is to determined,

$$\underline{\hat{\Phi}}_h(x) := \begin{pmatrix} \widehat{\Phi}_h^1(x) \\ \widehat{\Phi}_h^2(x) \end{pmatrix} = \sum_{j=1}^{M} \begin{pmatrix} \widehat{\Phi}_j^1 \\ \widehat{\Phi}_j^2 \end{pmatrix} \varphi_j^{(1)}(x) \in (\mathbb{S}_M^1 \cap \tilde{H}^{1/2}(\Gamma_N))^2 \quad \text{for } M < N$$

such that

$$\left\langle S\underline{\widehat{\Phi}}_h, \underline{v}_h \right\rangle_{\Gamma_N} = \langle \underline{u}_N + N\underline{g} - S\underline{\tilde{u}}_D, \underline{v}_h \rangle_{\Gamma_N} \quad \text{for all } \ \underline{v}_h \in (\mathbb{S}_M^1 \cap \tilde{H}^{1/2}(\Gamma_N))^2. \tag{6.5}$$

The unique solvability of the Galerkin formulation (6.5) can easily be derived as well as the following error estimates

$$\|\underline{\widehat{\Phi}} - \underline{\widehat{\Phi}}_h\|_{(H^{1/2}(\Gamma))^2} \leq ch^{3/2} |\underline{\widehat{\Phi}}|_{(H^2_{pw}(\Gamma))^2} \quad \text{and} \quad \|\underline{\widehat{\Phi}} - \underline{\widehat{\Phi}}_h\|_{(L^2(\Gamma))^2} \leq ch^2 |\underline{\widehat{\Phi}}|_{(H^2_{pw}(\Gamma))^2}, \tag{6.6}$$

for $\underline{\widehat{\Phi}} \in (H^2_{pw}(\Gamma))^2$. Additionally, From Galerkin's formulation (6.5), we derive the system of linear equations

$$\tilde{S}_h \underline{\tilde{\Phi}} = \underline{L}_1 + \underline{L}_2, \tag{6.7}$$

where

$$\tilde{S}_h := \mathbf{D}_h + (\frac{1}{2}\mathbf{M}_h^\top + \mathbf{K}_h^\top)\mathbf{V}_h^{-1}(\frac{1}{2}\mathbf{M}_h + \mathbf{K}_h), \tag{6.8}$$

is the stiffness matrix with $\mathbf{M}_h$ and $\mathbf{M}_h^\top$ denote the mass matrix and its transpose defined by

$$\mathbf{M}_h = \begin{pmatrix} \mathbf{M} & 0 \\ 0 & \mathbf{M} \end{pmatrix} \text{ with } \mathbf{M}[i,j] = \left(\int_\Gamma \varphi_j^{(1)} \cdot \varphi_i^{(0)} ds \right)_{i,j=1}^{M}.$$

Note that the matrices $\mathbf{D}_h$, $\mathbf{K}_h$, $\mathbf{V}_h$ and $\mathbf{V}_h^{-1}$ can be computed exactly (i.e., without being approximated) and efficiently, see [16, 17]. In addition, the FFT enables efficient computation of matrix-vector products with the inverse matrix $\mathbf{V}_h^{-1}$. Next, the right hand side of Eq. (6.7) is given by

$$\underline{L}_1[\ell] = \langle \underline{u}_N - S\underline{\tilde{u}}_D, \varphi_\ell^{(1)} \rangle_{\Gamma_N} \ \text{ and } \ \underline{L}_2[\ell] = \langle N\underline{g}, \varphi_\ell^{(1)} \rangle_{\Gamma_N} \quad \text{for } \ell = 1, ..., M.$$

To compute the Newton potential, let us consider the following decomposition of the fundamental solution

$$U_{11}^*(x,y) = U_{11}^{*1}(x,y) + U_{11}^{*2}(x,y), \quad U_{22}^*(x,y) = U_{11}^{*1}(x,y) - U_{11}^{*2}(x,y) \ \text{ and } \ U_{12}^*(x,y) = U_{21}^*(x,y) \tag{6.9}$$

with

$$\begin{cases} U_{11}^{*1}(x,y) = \alpha \log|x-y| + \dfrac{\beta}{2}, \\ U_{11}^{*2}(x,y) = \dfrac{\beta}{2} \dfrac{(x_1-y_1)^2 - (x_2-y_2)^2}{|x-y|^2}, \\ U_{12}^*(x,y) = \beta \dfrac{(x_1-y_1)(x_2-y_2)}{|x-y|^2} \end{cases} \tag{6.10}$$

such that

$$U^* = \begin{pmatrix} U_{11}^{*1} + U_{11}^{*2} & U_{12}^* \\ U_{12}^* & U_{11}^{*1} - U_{11}^{*2} \end{pmatrix}. \tag{6.11}$$

The vector of the volume potential for $m = 1, 2$, $\ell = 1, ..., N$ is given by:

$$\begin{aligned} (N_0\underline{g})_m[\ell] &= \sum_{k=1}^{M_r} \sum_{j=1}^{N} \int_{T_{kj}} \left[\int_{\tau_\ell} \left(g_1(y) U_{m1}^*(x,y) + g_2(y) U_{m2}^*(x,y) \right) ds_x \right] dy, \\ &= \sum_{k=1}^{M_r} \sum_{j=1}^{N} \sum_{p=1}^{2} \int_{\bar{T}_{kj}} \left[|J_\psi(\varepsilon,\lambda)| g_p(\psi(\varepsilon,\lambda)) \int_{\tau_\ell} U_{mp}^*(x, \psi(\varepsilon,\lambda)) \, ds_x \right] d\varepsilon d\lambda, \end{aligned} \tag{6.12}$$

where $|J_\psi(\varepsilon,\lambda)|$ is the Jacobian.

We can approximate (6.12) by

$$(\tilde{N}_0\underline{g})_m[\ell] = \sum_{k=1}^{M_r}\sum_{j=1}^{N}\sum_{i=1}^{\mathcal{I}}\left[w_{kj}^i|J_\psi(\varepsilon_i,\lambda_i)|\Big(\sum_{p=1}^{2}\big(\Pi_h g\big)_p\big(G_{kj}^i\big)\int_{\tau_\ell}U_{mp}^*\big(x,G_{kj}^i\big)\ ds_x\Big)\right], \tag{6.13}$$

for $\ell = 1,...,N$ and $m = 1,2$, where Π_h, w_{kj}^i and G_{kj}^i represent the interpolation operator, the weight and the point for the Gauss quadrature respectively. By permuting the second and third sum, (6.13) takes the following matrix form

$$\underline{\tilde{N}}_0\underline{g} = \sum_{k=1}^{M_r}\sum_{i=1}^{\mathcal{I}}\left[\begin{pmatrix}A_0^{ki} & 0\\ 0 & A_0^{ki}\end{pmatrix}+\begin{pmatrix}A_c^{ki} & A_{12}^{ki}\\ A_{12}^{ki} & -A_c^{ki}\end{pmatrix}\right]\begin{pmatrix}\underline{L}_1^{ki}\\ \underline{L}_2^{ki}\end{pmatrix}, \tag{6.14}$$

where A_0^{ki} for $k = 1,...,M_r$, $i = 1,...,\mathcal{I}$ is a circulant matrix and we have

$$A_0^{ki}[\ell,j] = \int_{\tau_\ell}U_{11}^{*1}(x,G_{kj}^i)ds_x,\quad A_c^{ki}[\ell,j] = \int_{\tau_\ell}U_{11}^{*2}(x,G_{kj}^i)ds_x,\quad A_{12}^{ki}[\ell,j] = \int_{\tau_\ell}U_{12}^{*}(x,G_{kj}^i)ds_x,$$
$$\underline{L}_m^{ki}[j] = w_{kj}^i|J_\psi(\varepsilon_i,\lambda_i)|\Pi_h g_m(G_{kj}^i)\qquad \text{for } m = 1,2,\ \ell,j = 1,...,N.$$

Note that the errors (4.18) and (4.19) remain valid in this case.

6.2. **Numerical examples.** For the numerical examples we consider the problem (6.1), where Ω is a circular domain centered at $c = (0.4,0.4)^\top$ with radius $R = 0.4$. We choose the boundary Γ_N as $\Gamma_N := \big\{(x_1,x_2)\in\mathbb{R}^2 : (x_1,x_2)^\top = (0.4+R\cos 2\pi\eta\ ,\ 0.4+R\sin 2\pi\eta)^\top,\ 0\le\eta\le 7/16\big\}$, and $\Gamma_D = \Gamma\backslash\Gamma_N$. Further, we use the Lamé constants $\lambda = 7142.86$ and $\mu = 1785.7$ for the material properties. In addition, we take

$$\underline{g}(x_1,x_2) = \begin{pmatrix}-6(2\mu+\lambda)x_1\\ -6(2\mu+\lambda)x_2+2\mu\end{pmatrix},$$

and the exact solution is

$$\underline{\Phi}(x_1,x_2) = \begin{pmatrix}x_1^3+x_2\\ -x_1^2+x_2^3\end{pmatrix}.$$

We first compute the vector of Newton potential $\underline{w} = V^{-1}(N_0\underline{g})$ which is needed in the right hand side of the linear system (6.7), see the Table 4 below.

TABLE 4. Time to compute $\underline{w} = V^{-1}(N_0\underline{g})$ with two (02) different methods.

Time to compute $\underline{w} = V^{-1}(N_0\underline{g})$			
N	M_r	By computing with FFT	By using direct method
64	11	0.25484	0.734
128	21	1.85167	5.58
256	41	14.72	43.77
512	82	114.84	351.12
1024	163	925.86	2870.51

In Table 4, the first and second columns list the number of elements and rings respectively. The column three represents the time to compute the vector $\underline{w} = V^{-1}(N_0\underline{g})$ by using the decomposition of the inverse of the single layer matrix given in [17, p.10], the decomposition of the vector $\tilde{N}_0\underline{g}$ given in formula (6.14) and the FFT while the last column contains the time to compute the vector $\underline{w} = V^{-1}(N_0\underline{g})$ by using the direct method. We can remark that at each level of refinement the time for the direct method is three times the time of the first method.

Finally, the linear system (6.7) is solved by the Conjugate gradient (CG) methods with preconditioner and without preconditioner. The results are presented in Table 5.

In Table 5, the third and the fourth columns represent the number of iterations for the CG method with preconditioner (#iter1) and the CG method without preconditioner (#iter2) respectively. The L^2 norms of $\underline{\Phi}-\underline{\Phi}_h$ and $\underline{t}-\underline{t}_h$

TABLE 5. The L^2 errors, estimate order of convergence and number of iterations.

		Iterations		L^2 **error of** $\underline{\Phi}$ **and eoc.**		L^2 **error of** $\underline{t} = T_x\underline{\Phi}$ **and eoc.**	
N	M_r	#iter1	#iter2	$\|\underline{\Phi} - \underline{\Phi}_h\|_{(L^2(\Gamma))^2}$	eoc	$\|\underline{t} - \underline{t}_h\|_{(L^2(\Gamma))^2}$	eoc
64	11	16	25	7.84×10^{-4}		440.83	
128	21	16	37	1.9987×10^{-4}	1.9718	220.396	1.00012
256	41	17	54	5.046×10^{-5}	1.9860	110.195	1.000039
512	82	17	78	1.2676×10^{-5}	1.9930	55.0968	1.000018
1024	163	17	111	3.1767×10^{-6}	1.9965	27.5483	1.000005
The expected theoretical results					**2**		**1**

are given respectively by the fifth and the seventh columns while the sixth and eight columns give the estimate order of convergence which converge to the results expected from theory.

CONCLUSION

In this article, the boundary element method and FFT method are used to present a fast and efficient resolution of the MBVP for the Poisson equation and the MBVP for the linear nonhomogeneous elasticity problem in two dimensional case. Our objective was based first on the efficient and fast computation of the Newton Potential and then on the analysis of the L^2 norm errors of the solutions and the estimated order of convergence. To achieve our goal, the Gauss-Hammer method and Gauss quadrature rule method are used to compute the Newton potential vector by considering a suitable discretization of the domain Ω, which has the configuration of a disc. Similarly, error minimization has been achieved using efficient and accurate computation of the matrices for the discrete boundary integral operators and application of the FFT method for solving the linear systems. Numerical examples are presented for both problems and the results we obtained show the accuracy, the efficiency and how powerful are our algorithms.

Our upcoming research will aim to extend these algorithmics techniques for the resolution of the mixed boundary value problem of the Poisson equation as well as the linear nonhomogeneous elasticity equation in three-dimensional on the spherical domain.

CONFLICTS OF INTEREST

The authors declare no competing interests.

REFERENCES

[1] M. Abbaszadeh, A. Ghoreyshi, and M. Dehghan, *A Finite Block Method Framework for Nonlinear Fractional Integro-Differential Equations*, Math. Meth. in the Appl. Sci., *0* (2025) 1–19.
[2] L. Coppolino and L. Desiderio, *Space-time energetic Galerkin BEM for the numerical solution of 3D elastodynamic problems: overcoming challenges of the strongly singular integral operator*, Comput. Mech. (2025).
[3] L. Desiderio, G. A. D'Inverno, M. L. Sampoli, and A. Sestin, *Hierarchical matrices for 3D Helmholtz problems in the multi-patch IgA-BEM setting*, Engineering with Computers, *41* (2025), 2021–2042.
[4] F. Ethridge and L. Greengard, *A new fast-multipole accelerated Poisson solver in two dimensions*, SIAM J. Sci. Comput., *23* (2001), 741–760.
[5] S. Falletta, G. Monegato, and L. Scuderi, *A space-time BIE method for nonhomogeneous exterior wave equation problems. The Dirichlet case*, IMA J. Numer. Anal., *32* (2012), 202–226.
[6] L. Gaul, M. Kogl, and M. Wagner, *Boundary Element Methods for Engineers and Scientists*, Springer, Heidelberg, 2003.
[7] A. Ghoreyshi, M. Abbaszadeh, M. A. Zaky, and M. Dehghan, *Finite block method for nonlinear time-fractional partial integro-differential equations: Stability, convergence, and numerical analysis*, Appl. Numer. Math., *214* (2025) 82–103.

[8] M. A. Golberg and C. S. Chen, *The theory of radial basis functions applied to BEM for inhomogeneous partial differential equations*, Bound. Elem. Comm., *5* (1994), 57–61.
[9] G. C. Hsiao, P. Kopp, and W. L. Wendland, *Some Applications of a Galerkin-collocation method for integral equations of the first kind*, Math. Methods Appl. Sci., *6* (1984), 280–325.
[10] G. C. Hsiao, P. Kopp, and W. L. Wendland, *A Galerkin collocation method for some integral equations of the first kind*, Computing, *25* (1980), 89–130.
[11] M. Jung and O. Steinbach *A finite element–boundary element algorithm for inhomogeneous boundary value problems*, Computing, *68* (2002), 1–17.
[12] J. Li, J. Z. Liu, T. Korakianitis, and P. H. Wen, *Finite block method in fracture analysis with functionally graded materials*, Eng. Anal. Boundary Elem., *82* (2017) 57–67.
[13] Y. Liu, L. Shen, and M. Bapat, *Development of the Fast Multipole Boundary Method for Acoustic Wave Problems*, In Recent Advances in Boundary Element Methods (G. D. Manolis, D. Polyzos eds.), Springer, 2009, 287–303.
[14] Z. D. Luo, *Finite Element and Reduced Dimension Methods for Partial Differential Equations*, Springer, Singapore, 2024.
[15] L. O. Ndjansi, *Mathematical analysis and numerical resolution of contact problems: combined penalization, semi-smooth Newton and boundary element methods*, 2025. Thesis (Ph.D.)–University of Dschang, Cameroon.
[16] L. O. Ndjansi, L. Tchoualag, and J. L. Woukeng, *Efficient numerical methods to approach solutions of quasi-static contact problems*, Results in Applied Math., *25* (2025) 100535.
[17] L. O. Ndjansi and L. Tchoualag, *An efficient computation of the inverse of the single layer matrix for the resolution of the linear elasticity problem in BEM*, Adv. Comput. Math., *49* (31) (2023).
[18] G. Of, O. Steinbach, and P. Urthaler, *Fast evaluation of volume potentials in boundary Element methods*, SIAM J. Sci. Comp., *32* (2010), 585–602.
[19] G. Of, O. Steinbach, and W. L. Wendland, *The fast multipole method for the symmetric boundary integral formulation*, IMA J. Numer. Anal., *26* (2006), 272–296.
[20] G. Of, O. Steinbach, and W. L. Wendland, *Applications of a fast multipole Galerkin boundary element method in linear elastostatics*, Comput. Vis. Sci., *8* (2005), 201–209.
[21] P. W. Partridge, C. A. Brebbia, and L. C. Wrobel, *The dual reciprocity boundary element method*, International Series on Computational Engineering, Computational Mechanics Publications, Southampton, 1992.
[22] S. Rjasanow and O. Steinbach, *The Fast Solution of Boundary Integral Equations*, Mathematical and Analytical Techniques with Applications to Engineering, Springer, New York, 2007.
[23] O. Steinbach and L. Tchoualag, *Fast Fourier transform for efficient evaluation of Newton potential in BEM*, Appl. Num. Math., *81* (2014), 1–14.
[24] O. Steinbach, *Numerical Approximation Methods for Elliptic Boundary Value Problems*, Finite and Boundary Elements, Springer, New York, 2008.
[25] O. Steinbach, *Fast evaluation of Newton potentials in boundary element methods*, East-West J. Numer. Anal., *7* (1999), 211–222.
[26] L. Tchoualag, L. O. Ndjansi, J. D. Mukam, and A. Tambue, *Boundary element method for Laplace equation in a ring domain*, Partial Differential Equations in Applied Mathematics, *17* (2026), 101334.
[27] L. Tchoualag, L. O. Ndjansi, and J. L. Woukeng, *Rapid Methods for the Resolution of Contact Problems in Static Linear Elasticity*, Math. Prob. Eng., *2023* (2023), Article ID 9960116, 1-26.